JOINT CENTER FOR SATELLITE DATA ASSIMILATION

NO. 65, Fall 2019

JCSDA Quarterly

NOAA | NASA | US NAVY | US AIR FORCE

https://doi.org/10.25923/ttpr-1d55

IN THIS ISSUE

Contents

NEWS IN THIS QUARTER

Prediction and Data Assimilation for Cloud (PANDA-C)

Introduction

Clouds significantly impact numerous military operations. Even as new technology has improved the resolution and precision of warfighting capabilities, those same technologies carry with them the requirement for better temporal and spatial resolution of smaller atmospheric constituents down to the individual cloud elements. For example, low cloud cover and ceilings can enhance some military operations by providing low-level cover and concealment. However, the inability for aircrews or increasingly sensitive target acquisition software to identify targets through cloud layers can be detrimental. In addition, poor surface visibility due to clouds or fog can negatively impact aircraft takeoffs and landings. Finally, the need to anticipate/exploit cloud impacts on remotely piloted aircraft (RPA) is paramount when controlling these capabilities thousands of miles from the area of operation. These traditional and emerging requirements have driven Air Force Weather in pursuit of the most accurate cloud analyses and forecasts possible.

Continued improvements are needed to drive Air Force Weather cloud characterization capabilities toward greater resolution, improved vertical and horizontal fidelity, and reduced latency to meet current and future requirements from DoD communities. Explicit numerical weather prediction (NWP)-based cloud prediction with direct satellite radiance assimilation may offer a solution and allow a unified modeling approach. Such a unified modeling approach will simplify Air Force Weather's computational infrastructure (software and hardware), eliminate duplication of effort, and optimize our application of resources.

The U.S. Air Force is currently funding the National Center for Atmospheric Research (NCAR) and the Joint Center for Satellite Data Assimilation (JCSDA) to research and produce a cloud data assimilation system to allow for better cloud forecasts explicitly represented in our modeling system. This effort, Prediction and Data Assimilation for Cloud (PANDA-C), is led by Chris Snyder, Jake Liu, and Tom Auligné. NCAR has worked on this project in partnership with the JEDI core team at JCSDA and the United Kingdom Met Office (UKMO).

Disclaimer: *The manuscript contents are solely the opinions of the author(s) and do not constitute a statement of policy, decision, or position on behalf of NOAA or any other JCSDA partner agencies or the U.S. Government.*

JOINT CENTER FOR SATELLITE DATA ASSIMILATION

5830 University Research Court
College Park, Maryland 20740

3300 Mitchell Lane
Boulder, Colorado 80301

Website: www.jcsda.org

EDITORIAL BOARD

Editor:
James G. Yoe

Assistant Editor:
Biljana Orescanin

Director:
Thomas Auligné

Chief Administrative Officer:
James G. Yoe

Support Staff:
Sandra L. Claar

PANDA-C

Most of the development under PANDA-C is within the Joint Effort for Data assimilation Integration (JEDI). JEDI is data-assimilation software and development practices that allow JCSDA partners and other groups to collaborate effectively in building state-of-the-art assimilation systems for a variety of forecast models and physical problems. The team is working with the Model for Prediction Across Scales (MPAS) and the UKMO's LFRic in parallel as it designs JEDI interfaces for assimilation data relevant to cloud analysis and forecasting.

NCAR has experience in data assimilation using MPAS, and it was chosen as a development platform for PANDA-C. LFRic was chosen as it is the next generation UKMO model, and since the Air Force operates a UKMO-based system today that provides a path forward for future Air Force/UKMO partnership. Even though these models have been chosen for this initial development, the JCSDA separation of concerns approach will allow the JEDI-based system to be agnostic of the choice of dynamic model in the long term.

The past year has seen rapid development of MPAS-JEDI, which is the term that refers to the assimilation system employing the MPAS model, the MPAS interfaces to JEDI and the other JEDI components. That development has occurred in MPAS-specific elements of JEDI and also within other aspects of JEDI.

For MPAS-JEDI, NCAR developed two prototypes of the MPAS model interfaces. The first was based on experience from other data-assimilation research with MPAS (Ha et al. 2017) and allowed NCAR to gain experience with object oriented programming systems (OOPS) and to begin immediately developing and exercising all parts of the system necessary for cycling data-assimilation experiments. In the second, NCAR revised the choice of analysis variables to reduce the nonlinearity of the observation-state relations and to facilitate development of a generic background-covariance capability between atmospheric models in JEDI, including LFRic.

The second, MPAS-JEDI Prototype II, has been tested with cycling assimilation for a full month (more than 100 6-h cycles) and using an initial parallel implementation that runs on multiple processors on NCAR's high-performance computing. This is a significant accomplishment that was achieved one year ahead of schedule. Prototype II can assimilate: wind, temperature and specific humidity from radiosondes and aircraft, atmospheric motion vectors (AMVs), global navigation satellite system (GNSS)-radio occultation (RO) reflectivity/bending angle, and surface pressure. MPAS-JEDI can also assimilate satellite radiances with Community Radiative Transfer Model (CRTM), but have reached only partial utility with no bias correction or cloud detection. NCAR implemented a necessary MPAS-JEDI interface to those observation operators in UFO.

As part of broader MPAS-JEDI developments, PANDA-C work contributed to multiple additional aspects of JEDI. NCAR used B Matrix on Unstructured Mesh Package (BUMP) as the univariate covariance model in MPAS-JEDI. NCAR implemented translators that allow Interface for Observation Data (IODA) to ingest observations from UKMO files in ODB2 format and contributed to the initial IODA code for in-core observation storage. NCAR implemented a forward operator for surface pressure in the Unified Forward Operator (UFO), and more significantly, the associated correction for differences between the model terrain height and the observation's station elevation. In addition, PANDA-C funded staff on the JEDI core team have developed a prototype automated testing framework for JEDI. NCAR identified ways to increase computational efficiency in the system. NCAR also made substantial progress on assimilation of radiances from geostationary platforms in the context of WRF and WRFDA. Finally, NCAR executed a month-long cycling experiment with the MPAS-JEDI Prototype II, which is highlighted below.

Month-Long Cycling Experiment

Model configuration and experimental setup

MPAS-JEDI Prototype II is configured with a uniform 120-km grid spacing (total 40 962 cells) and 55 vertical levels with the model top at 30 km (~10 hPa). Three one-month, 6-hourly cycling runs are from 0000 UTC 15 Apr 2018 to 0000 UTC 14 May 2018. Sea surface temperature (SST) and sea ice coverage are updated every 6-h during cycling. MPAS-JEDI Prototype II data assimilation was tested for robustness and stability through cycling data assimilation and forecast experiments over a month-long period. The first trial of month-long cycling led to some failures after about 2 weeks cycling due to rapid drift of some fields, which was caused by a bug in variable transform of dry air density in the MPAS-JEDI interface. After this bug fix, the model is able to run one-month cycling and 10-day forecasts without failures.

Three experiments were conducted: 3DVar, pure 3DenVar, and hybrid-3DEnVar. One outer loop with maximum 75 iterations is used for the minimization of the cost function. 3DVar employed univariate static B via BUMP, which diagnosed variance and correlation scales from 20-member GEFS ensembles. For 3DEnVar and hybrid-3DEnVar, ensemble input is from 20-member GEFS 6-hour forecasts. The vertical localization radius is is set to five model levels and the hoirzontal localization radius is set to 2000 km. In hybrid-3DEnVar, static and ensemble part of B is assigned equal weight. The PREQC (threshold = 3) function was implemented in UFO, which assimilates the observations with QC flag (output from GSI ncdiag files) equal or less than 3. Background departure check is also performed for all observations. 10-day forecasts are conducted at each 00 UTC.

Observations

The observations assimilated in all the three experiments are from four observing networks, including radiosondes (U, V, T, Q), aircrafts (U, V, T, Q), AMVs (U and V), and GNSSRO (refractivity). One-month of these observations was converted to IODA-NC format using an IODA converter. For satellite AMVs, MPAS-JEDI uses the IODA random thinning function to keep 25% (tunable) of original. These observations are also used to verify the cycling results.

Results

Time series of OMB statistics: In ***Figure 1***, the model background (i.e., 6-h MPAS model forecast) U is verified against satellite AMVs for all vertical levels together. The number of observations used in three experiments decrease during the 1-month cycling run.

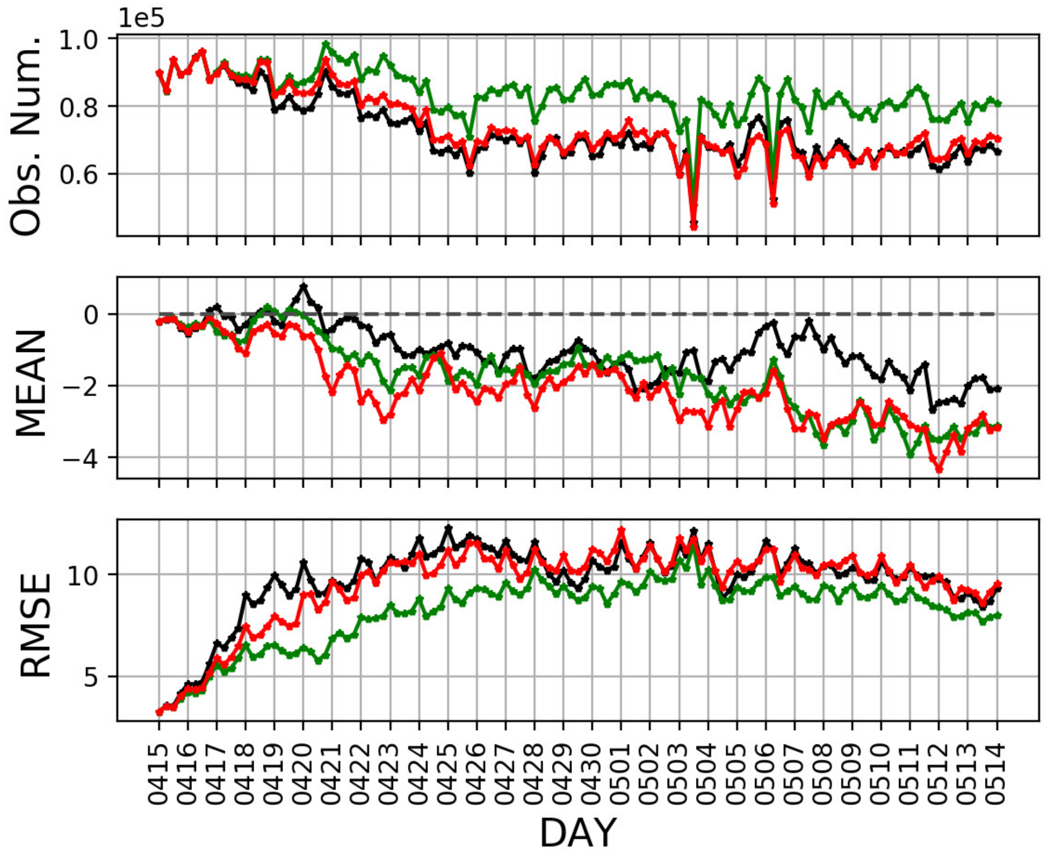

Figure 1. *Time series of the number of AMV's U used in data assimilation (top), Bias of OMB (middle), and RMS of OMB (bottom) over 1-month cycling period. Black: 3DVar; Green: 3DEnVar; Red: Hybrid.*

Apparently 3DEnVar overall outperforms 3DVAR and hybrid-3DEnVar, indicated by more observations assimilated and smaller RMS in 3DEnVar. 3DVAR worse than 3DEnVar is expected, but hybrid-3DEnVar not better than 3DEnVar is not expected. The latter may be related to the univariate nature of static B (i.e., no cross-correlation among different analysis variables). There is an obvious bias for the U wind with the background winds stronger than the observed AMVs after 1-week cycling for 3 experiments. For 3DVar and Hybrid, RMSE increased more than 5m/s after 1-week.

In ***Figure 2***, the model background temperature is verified against radiosonde observations. It shows that background T is colder than observation. The RMSE are around 1.6 K. There is a jump at 0600 UTC 30 Apr 2018. The reason is that only small number of observations can be used in verification procedure at this time. The 3DEnVar uses some more observations than the other two experiments during cycling run. However, 3DEnVar's T performance is not very different from 3DVar and Hybrid like for AMV's U.

Forecast verification: ***Figures 3*** and ***4*** show the 10-day forecast verification for U component from AMVs and T from radiosondes. 3DEnVar clearly outperformed 3DVar and Hybrid in terms of both mean bias and RMSE.

Conclusion

Much progress has been made, but there is much work yet to be done. NCAR plans to provide a cloud verification capability to

Figure 2. *Same as Figure 1 but for radiosonde T.*

measure PANDA-C progress in improving cloud forecasting. In addition, BUMP multivariate covariance will be examined. NCAR plans to continue to improve and test geostationary satellite all-sky IR radiance assimilation impact on cloud forecasts and assess its added benefit above clear-sky radiance assimilation from the same source. Depending on progress of MPAS-JEDI prototype development, some of the geostationary satellite assimilation could be ported into JEDI framework in year 2.

PANDA-C has achieved significant success implementing MPAS-JEDI and developing other aspects of the JCSDA ecosystem. In addition, progress on geostationary satellite radiance data assimilation has been made by the PANDA-C team. The U.S. Air Force welcomes these advances in cloud forecasting and looks forward to continued partnership with NCAR's PANDA-C team, JCSDA, and the UKMO moving forward.

Author

John McMillen

References

Ha, S., C. Snyder, W. C. Skamarock, J. Anderson, and N. Collins, 2017: Ensemble Kalman filter data assimilation for the Model for Prediction Across Scales (MPAS). *Monthly Weather Review*, 145, 4673-4692, doi:10.1175/MWR-D-17-0145.1.

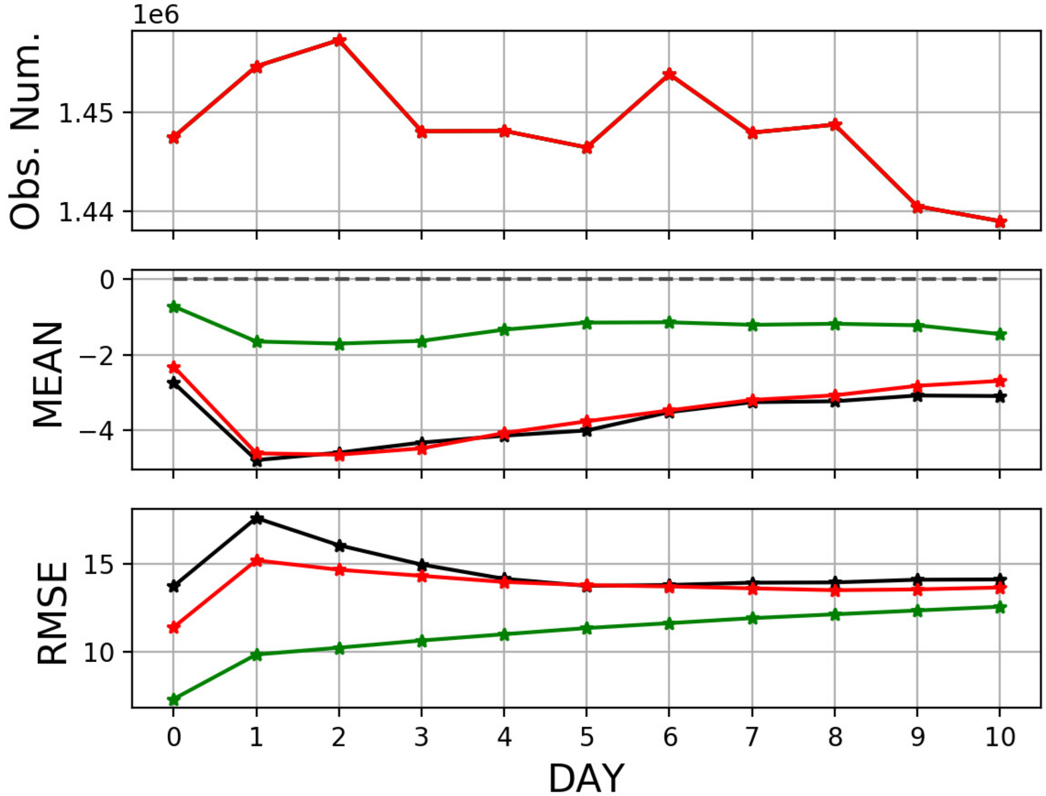

Figure 3. *Satellite U. MEAN and RMSE of 10-day forecast verified against U component of satellite AMVs over 20 days for 3DVar (black), 3DEnVar (green), and hybrid (red).*

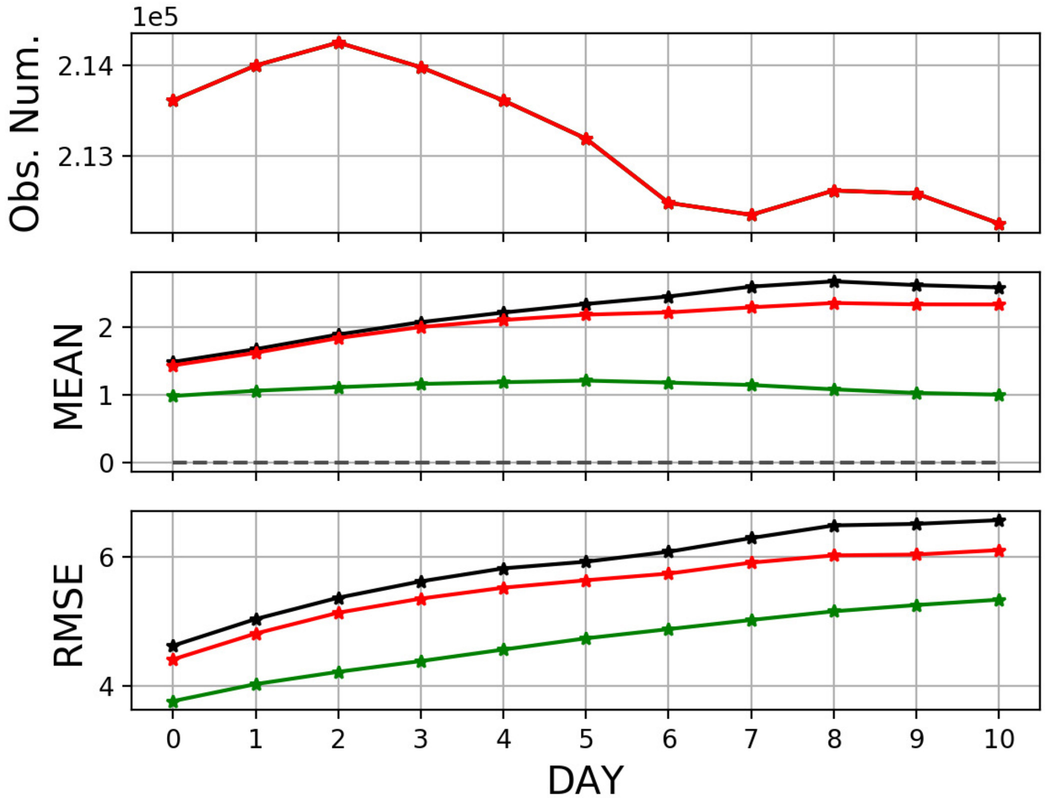

Figure 4. *Same as Figure 3 but for radiosonde T.*

Impact of Assimilating Adaptively Thinned AIRS Cloud-Cleared Radiances in the GEOS

The advent of hyperspectral infrared radiance assimilation from NASA's Atmospheric Infrared Sounder (AIRS) introduced a significant improvement in numerical weather prediction systems (Le Marshall et al., 2006). However, this improvement stems from the use of highly thinned, cloud-free radiances only, leaving valuable data in cloudy conditions underutilized. Despite the tremendous progress and success of assimilating all-sky microwave (MW) radiances, no operational center currently assimilates hyperspectral infrared radiances in cloudy conditions (Geer et al., 2018). An additional issue with infrared radiance assimilation, as it is currently performed, is the method of thinning. Due to computational costs associated with processing the vast volume of hyperspectral infrared data, operational thinning reduces data volume to a few percent of the total available (Goldberg et al., 2003; Chahine et al., 2006; McCarty et al., 2009). Thinning is performed on a homogeneous, uniform grid, leading to the undersampling of meteorologically active regions, characterized by rapid rates of change and sharp gradients (Ochotta et al., 2005; Lazarus et al., 2010; Reale et al., 2018).

Based on an extensive set of AIRS-focused data impact studies that showed an extreme sensitivity of Tropical Cyclones (TCs) to changes in data assimilation strategy, from both a data density and the use of information in cloudy regions perspective, Reale et al. (2018) proposed a simple solution. They advocated for a TC-centered adaptive assimilation of cloud-cleared radiances (CCRs) in the NASA Goddard Earth Observing System (GEOS). The adaptive thinning methodology adopted by Reale et al. (2018) consists of assimilating higher density AIRS radiances within a moving domain surrounding TCs identified by Best Track information, or alternatively by TC Vitals (Trahan and Sparling, 2012) in near real-time situations and assimilating lower density AIRS data elsewhere. By implementing this adaptive thinning methodology in the GEOS data assimilation system (DAS), in a 3D variational (3DVar) framework, they found that for the boreal fall of 2014, tropical cyclones were better represented in the analysis and forecast, while simultaneously producing a slight improvement to the 500-hPa geopotential height anomaly correlation relative to the quasi-operational system run by the Global Modeling and Assimilation Office (GMAO) at that time.

Highlights of Adaptive Thinning and Assimilating Cloud-cleared Radiances

More recent work has expanded the efforts of Reale et al. (2018) to examine the impact of 1) assimilating cloud-cleared AIRS radiances on the Arctic atmosphere, 2) a comprehensive adaptive thinning approach that incorporates not only AIRS radiances, but also those from the Cross-track Infrared Sounder (CrIS) and the Infrared Atmospheric Sounder Interferometer (IASI), and 3) the assimilation of cloud-cleared AIRS radiances within a hybrid 4D ensemble variational (hybrid 4DEnVar) framework.

Arctic and Mid-latitude Impacts

The Arctic region is extremely data scarce having few in situ observations, with an extensive presence of low-level stratus clouds limiting the assimilation of clear-sky only infrared radiances from satellites. Instead, by utilizing cloud-cleared radiances which may be obtained in partially cloudy regions, it is possible to assimilate satellite observations from within the broken stratus layer, providing valuable information content in this unique environment to the analysis. During the boreal fall 2014 (September 1, 2014 – November 10, 2014), using the same set of Observing System Experiments (OSEs) as described by Reale et al. (2018), the assimilation of lower density cloud-cleared AIRS radiances, relative to the assimilation of clear-sky radiances, results in slightly cooler but spatially consistent low-tropospheric temperatures in the analysis over the central Arctic Ocean (vertically integrated from the surface to 800-hPa in the time mean; ***Figure 1***). The negative temperature anomaly translates to a reduction in the mid-tropospheric height due to hydrostatic adjustment ***(Figure 2)***. These modifications are also evident in a time series of the areal mean, averaged poleward of 70°N, incorporating an area over 15 million square kilometers. The persistent cooling in the lower-tropospheric temperatures and associated lowering of the mid-tropospheric geopotential height are a remarkable consequence of assimilating cloud-cleared radiances rather than clear-sky ***(Figure 3)***.

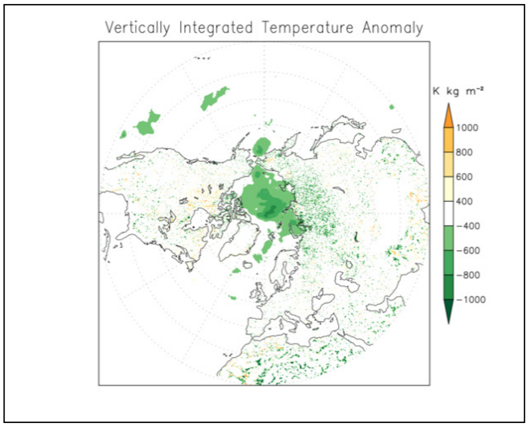

Figure 1. *Vertically integrated temperature anomaly (from the surface to 800-hPa) for the cloud-cleared minus clear-sky experiments temporally averaged from September 1 – November 10, 2014.*

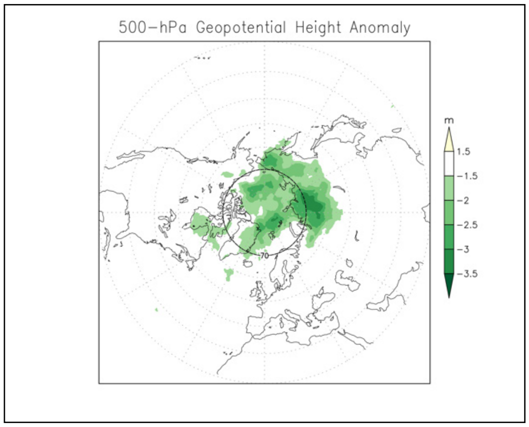

Figure 2. *The same as Figure 1 but for 500-hPa geopotential height.*

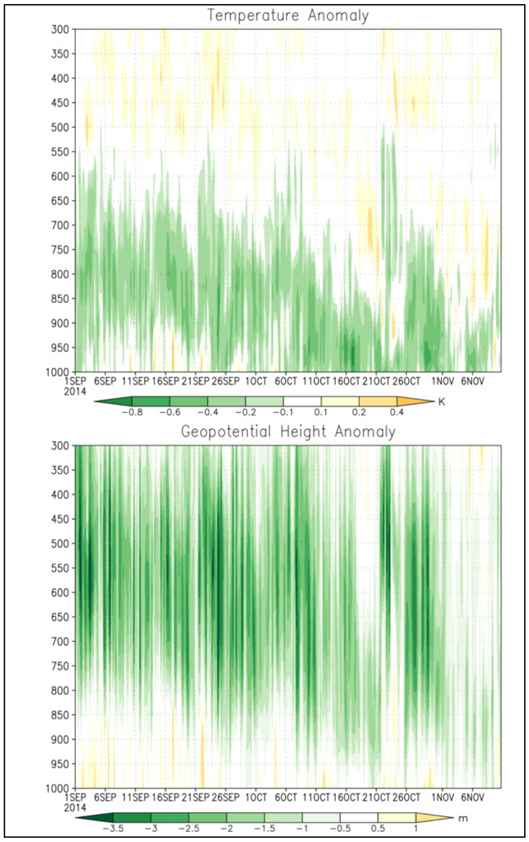

Figure 3. *Time height cross of temperature (top) and geopotential height (bottom) anomaly for the cloud-cleared minus clear-sky experiments averaged from 70°N poleward.*

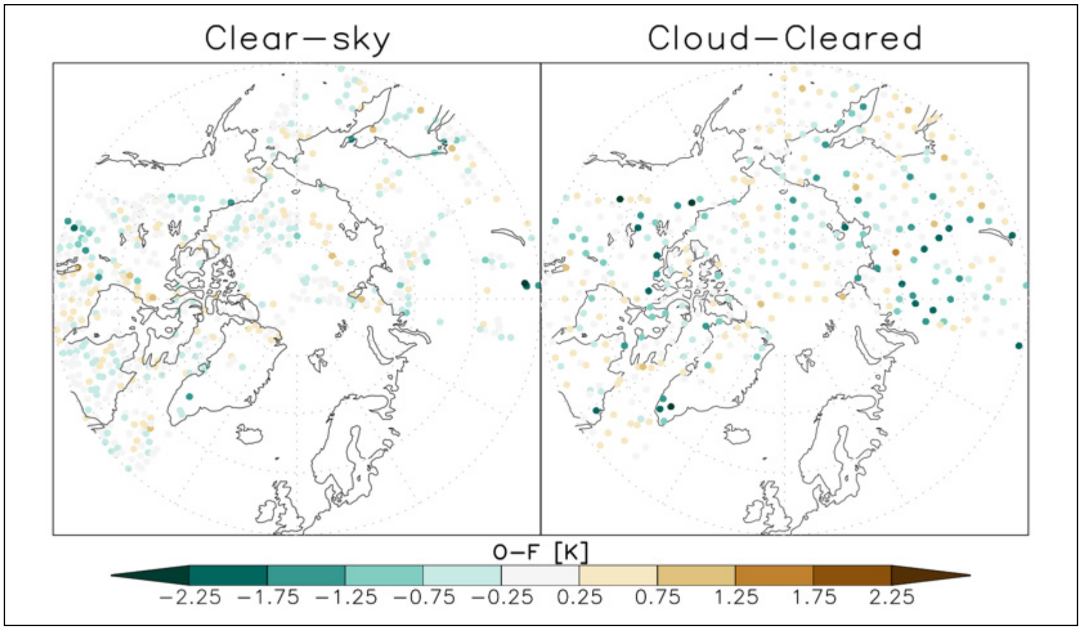

Figure 4. *AIRS radiance coverage at 18 UTC October 21, 2014. Circles indicate locations of assimilated radiances: O-F brightness temperatures (K), channel 169, corresponding to approximately 185 hPa.*

These effects in the analysis produce alterations in the corresponding forecasts. Specifically, in the clear-sky radiance assimilation case, large data voids occur ***(Figure 4)***, which propagate in poorly forecasted individual waves, to the point of affecting the skill for the entire hemisphere. The same waves, when initialized from analyses resulting from the assimilation of cloud-cleared radiances, are better forecasted so that the global skill responds positively. Even if these large data void situations are sporadic, their devastating effect on the skill is so strong that it persists into the monthly averages. In other words, the correction of individual, low-skill outlier forecasts, allowed by the assimilation of cloud cleared radiances, improves the global skill and forces individual wave prediction in the direction of the verifying analysis. An example of this large improvement is shown in ***Figure 5***.

Comprehensive Adaptive Thinning Approach

The assimilation of cloud-cleared AIRS radiances, at a reduced density resulting from a larger thinning box size, brings a substantial improvement in global forecast skill (compared to clear-sky), as measured by 500-hPa geopotential height anomaly correlation, due to the impact of the modified temperature structure on mid-latitude waves. However, without additional information in the vicinity of tropical cyclones, it has a negligible impact on TC structure. Adaptive thinning offers a good compromise for improving the representation of TCs without degrading global skill when assimilating cloud-cleared radiances (Reale et al., 2018). Therefore, in addition to the experiments focused on AIRS only, we now examine the impact

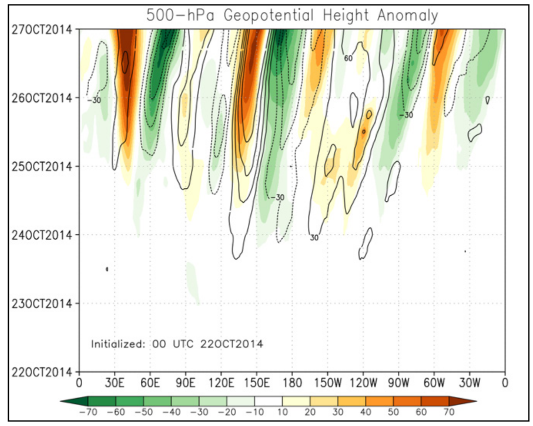

Figure 5. *Hovmöller diagram showing 500-hPa geopotential height anomaly for the cloud-cleared experiment forecast minus the clear-sky forecast averaged from 40°N to 80°N (shaded) and NCEP operational analysis minus the clear-sky forecast (contour), initialized from 00 UTC October 22, 2014.*

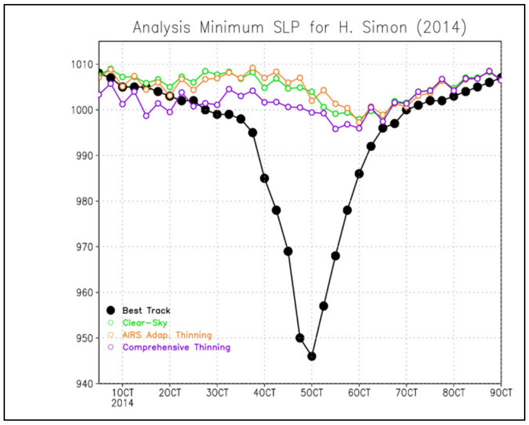

Figure 6. *Analysis of minimum center pressure for Hurricane Simon in various experiments and the Best Track.*

of a comprehensive adaptive thinning strategy applied to all hyperspectral infrared instruments together (AIRS, CrIS, and IASI). Since cloud-cleared CrIS and IASI radiances are not yet available for assimilation into the GEOS DAS, the IASI and CrIS clear-sky radiances were adaptively thinned, along with the cloud-cleared AIRS radiances, using the same methodology as the experiments examining AIRS alone.

This experiment resulted in a significant improvement in both global skill and TC representation. One notable difference between the comprehensive thinning approach and adaptive thinning of AIRS radiances alone is that when all instruments are considered together, TCs, which were difficult to represent with AIRS only, improve substantially. Specifically, some short-lived, small-scale TCs, whose life cycles were not adequately sampled by the AIRS swath alone, were much better resolved when data from all 3 instruments were adaptively thinned. By adaptively thinning the four sensors (there are two IASI instruments, onboard both MetOp-A and MetOp-B), several more of these 'difficult' TCs are positively affected. One particularly difficult to represent East Pacific storm, Hurricane Simon (October 1-7, 2014), was short-lived and characterized by rapid intensification (50 hPa in 36 hours) and rapid dissipation (50 hPa in 48 hours) over the course of less than four days (***Figure 6***; Stewart, 2014). The storm could not be represented in either the control or in experiments with adaptively thinned AIRS cloud-cleared radiances alone. The storm structure was unresolved, appearing as an open wave without any warm core. On the contrary, the comprehensive thinning approach produces an improvement, with a more compact warm core, higher wind speeds, slightly lower sea level pressure, and improved alignment ***(Figure 7)***. This improvement in the analyzed structure, even if modest, given the difficulty in analyzing such a short-lived storm, contributed to a substantial improvement in the 48-hour intensity forecast: the predicted intensity is comparable to forecasts generated from an analysis that included the vortex relocator. This indicates that assimilation of infrared hyperspectral data alone has the ability to effectively constrain TC storms' structure.

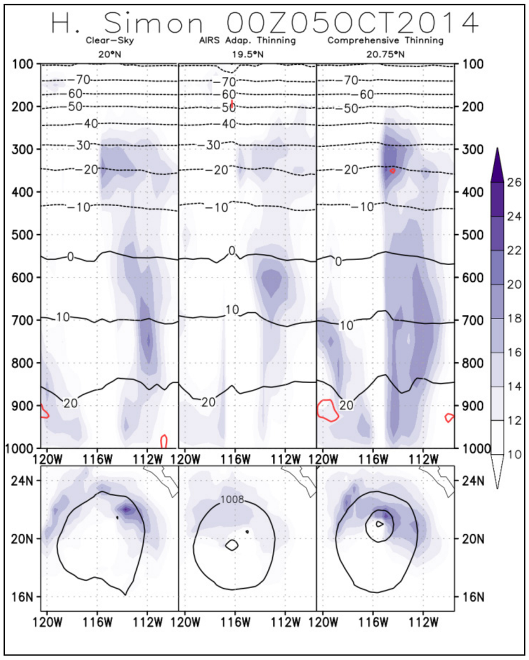

Figure 7. *Zonal vertical section of wind (m s-1), temperature (°C; solid black contours) and the temperature anomaly (solid red contours; contours every 2°C, only ≥2°C for clarity) for Hurricane Simon at 00 UTC October 5, 2014, comparing various experiments (top). Horizontal winds at 850-hPa (m s-1; shaded) and SLP (hPa; solid) (bottom).*

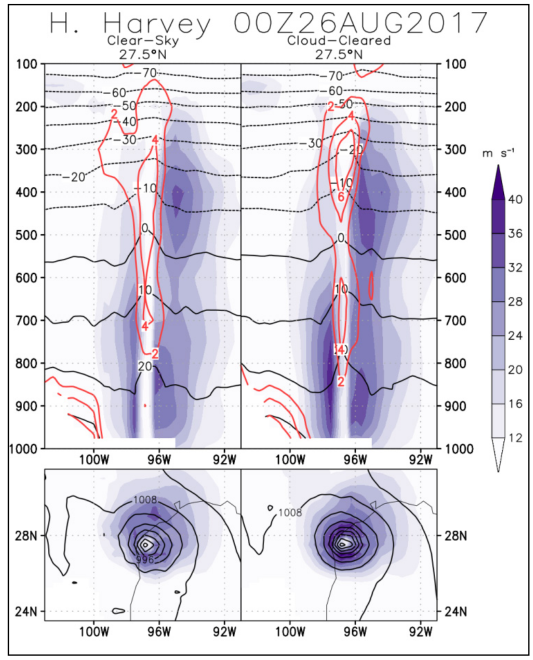

Figure 8. *Zonal vertical section of wind (m s-1), temperature (°C; solid black contours) and the temperature anomaly (solid red contours; contours every 2°C, only ≥2°C for clarity) for Hurricane Harvey at 00 UTC August 26, 2017, comparing various experiments (top). Horizontal winds at 850-hPa (m s-1; shaded) and SLP (hPa; solid) (bottom).*

Experiments Using Hybrid 4DEnVar

Given the positive results found from using adaptive thinning and the use of cloud-cleared AIRS radiances in a 3DVar framework, work has begun on transitioning to a hybrid 4DEnVar framework, taking advantage of the assimilation updates being added hourly. Similar to the 3DVar experiments, the largest impact of assimilating cloud-cleared AIRS radiances, rather than clear-sky, occurs in the vicinity of tropical cyclones. This is due to the ability to assimilate cloud-cleared radiances in partially-cloudy regions, particularly within the rain bands of TCs, providing information in a previously undersampled and rapidly changing environment with large gradients. The impact on the tropical cyclone scale is attributable to a better representation of the temperature dipole on top of a TC (with warmer temperatures within the core of the storm and cooler temperatures in the surrounding environment). This leads to a deepening of the storm, due to hydrostatic adjustment. In the hybrid 4DEnVAR framework, the assimilation of cloud-cleared radiances with homogeneous data density (without adaptive thinning) can improve not only the global skill but also the representation of TCs, unlike the 3DVAR experiments. Hurricane Harvey, a TC that affected the United States Gulf Coast in August 2017, was better represented due to additional information in cloudy regions because of the assimilation of cloud-cleared radiances rather than clear-sky. In the analysis, the warm core structure was improved with stronger wind speeds and lower sea level pressure accompanied by an overall improved vertical and horizontal structure ***(Figure 8)***. These positive effects resulted in an improved intensity and track forecast for this devastating storm, relative to the assimilation of clear-sky radiances. It is expected that the incorporation of adaptive thinning of these radiances, as well as the use of cloud-cleared CrIS and IASI radiances, will result in further improvements to TC structure and forecast and for additional storms.

Discussion

Currently, hyperspectral infrared data are suboptimally used within operational numerical weather prediction systems. Two major problems are homogenous thinning, which causes under- and over-sampling of meteorologically active and inactive regions, respectively, and the restriction to the assimilation of only channels unaffected by clouds. The first problem is connected to thinning performed through a regular grid, widely adopted to offset computational expense, and necessary because of the inherent complexity of theoretical frameworks designed to optimize data density. The second problem is connected to the loss of extremely valuable information that occurs when the assimilation of hyperspectral infrared radiances is restricted to clear-sky conditions. Both of these issues become particularly evident in the analyzed representation of tropical cyclones because of the exceptionally strong and concentrated horizontal gradients, and the extensive cloud cover, which dramatically limits the amount of information provided by clear-sky data of the spatiotemporal structure of the storm.

Reale et al., (2018) showed that a simple, TC-centered adaptive thinning methodology of assimilating cloud-cleared infrared radiances from AIRS is capable of improving the representation of tropical cyclones, without degrading the global forecast skill. More recent work has shown that the slight improvement in global forecast skill when using uniform but lower density cloud-cleared radiances is likely to be induced by the strong sensitivity of the Arctic region to the assimilation of cloud-cleared radiances, which provide valuable information within otherwise data void, broken stratus cloud areas. This impacts the representation of central Arctic lower-tropospheric dynamics, which then improves the forecast of some mid-latitude waves, particularly the ones originating in data void areas, through adjustments to the mid-tropospheric geopotential height. A further improvement can be obtained by using a comprehensive thinning approach, meaning the use of an adaptive thinning methodology on all available hyperspectral infrared radiances, AIRS, CrIS, and IASI. This produces an improvement in the global forecast skill and an even better TC representation in the analysis and forecast than was capable by adaptively thinning AIRS radiances alone (Reale et al., 2018). Additional experiments, extending the use of cloud-cleared AIRS radiances to the hybrid 4DEnVar version of the GEOS DAS, show encouraging results and confirm the strong sensitivity of TC representation to CCR assimilation. This outcome encourages the continued investigation of cloud-cleared hyperspectral infrared radiances in an adaptive thinning methodology.

Authors

Erica L. McGrath-Spangler
Universities Space Research Association (USRA)/Goddard Earth Sciences Technology and Research (GESTAR), NASA Global Modeling and Assimilation Office (GMAO)

Oreste Reale
Universities Space Research Association (USRA) Goddard Earth Sciences Technology and Research (GESTAR), NASA Global Modeling and Assimilation Office (GMAO)

Manisha Ganeshan
Universities Space Research Association (USRA) Goddard Earth Sciences Technology and Research (GESTAR), NASA Climate and Radiation Laboratory

Will McCarty
NASA Global Modeling and Assimilation Office (GMAO)

Ron Gelaro
NASA Global Modeling and Assimilation Office (GMAO)

References

Chahine, M. T., et al. (2006), AIRS: Improving weather forecasting and providing new data on greenhouse gases, Bull. Am. Meteorol. Soc., 87(7), 911–926, doi:10.1175/BAMS-87-7-911.

Geer, AJ, K. Lonitz, P. Weston, et al. (2018), All-sky satellite data assimilation at operational weather forecasting centres, Q J R Meteorol Soc., 144, 1191–1217, https://doi.org/10.1002/qj.3202.

Goldberg, M. D., Y. Qu, L. M. McMillin, W. Wolf, Z. Lihang, and M. Divakarla (2003), AIRS near-real-time products and algorithms in support of operational numerical weather prediction, IEEE Trans. Geosci. Remote Sens., 41(2), 379–389, doi:10.1109/TGRS.2002.808307.

Lazarus, S. M., M. E. Splitt, M. D. Lueken, and B. T. Zavodsky, (2010), Evaluation of data reduction algorithms for real-time analysis. Wea. Forecasting, 25, 837–851, https://doi.org/10.1175/2010WAF2222296.1.

Le Marshall, J., et al. (2006), Improving global analysis and forecasting with AIRS, Bull. Am. Meteorol. Soc., 87(7), 891–894, doi:10.1175/BAMS-87-7-891.

McCarty, W., G. Jedlovec, and T. L. Miller, (2009), Impact of the assimilation of Atmospheric Infrared Sounder radiance measurements on short-term weather forecasts. J. Geophys. Res., 114, D18122, https://doi.org/10.1029/2008JD011626.

Ochotta, T., C. Cebhardt, D. Saupe, and W. Wergen, (2005), Adaptive thinning of atmospheric observations in data assimilation with vector quantization and filtering methods. Quart. J. Roy. Meteor. Soc., 131, 3427–3437, https://doi.org/10.1256/qj.05.94.

Reale, O., E.L. McGrath-Spangler, W. McCarty, D. Holdaway, and R. Gelaro, (2018), Impact of Adaptively Thinned AIRS Cloud-Cleared Radiances on Tropical Cyclone Representation in a Global Data Assimilation and Forecast System. Wea. Forecasting, 33, 909–931, https://doi.org/10.1175/WAF-D-17-0175.1.

Stewart, S. R., (2014), Hurricane Simon (EP192014), 1–7 October 2014. National Hurricane Center Tropical Cyclone Rep., 18 pp., https://www.nhc.noaa.gov/data/tcr/EP192014_Simon.pdf

Trahan, S., and L. Sparling, (2012), An analysis of NCEP tropical cyclone vitals and potential effects on forecasting models. Wea. Forecasting, 27, 744–756, https://doi.org/10.1175/WAF-D-11-00063.1.

Advances in Land Surface Microwave Emissivity Modeling

Introduction

Satellite observations of microwave sounding channels have been extensively utilized in numerical weather predictions (NWP) to improve the analysis of atmospheric state variables (e.g., vertical temperature and water vapor profiles) and the overall forecasting skills of the NWP system. Very few microwave observations of surface sensitive and window channels are assimilated in the data assimilation over the land surfaces. They are basically used as ancillary information supporting the quality control and thinning of the associated sounding channel observations. Amongst all those possible limiting factors, the lack of fully functional surface emissivity models should be one of the primary.

In the current operational Community Radiative Transfer Model (CRTM), the microwave (MW) land surface emissivity is calculated with a three-medium-layer two-stream radiative transfer model (Weng et al. 2001, Chen et al. 2016). The top layer and the bottom layer are air and soil, respectively. The middle layer depends on land surface cover types, which may be vegetation canopy or snow. Volumetric scattering of the middle layer and the reflection at medium interfaces are considered. Since the MW land emissivity model is based on generic radiative transfer theory, it may be applied for any sensors within the model validity range. More importantly, the MW physical land surface emissivity model (MPLSEM) provides real-time response of surface emissivity to the changes of surface state variables. It allows sensitivity analysis of surface emissivity to each individual surface control variables. If the tangent-linear adjoint model is provided, the MPLSEM may be applied to improve the analysis of the surface state variables with the observations from satellite window channels, especially those of low frequency channels (e.g., SMAP L-band and AMESR-2 C-band to X-band).

Despite the advantage of the MPLSEM in theory, its practical application has been very challenging due to insufficient model calibration at global scale and the uncertainties involved in the model inputs. The MPLSEM is found to have limited capability to characterize the spatial variations of each different surface cover types, resulting in very inefficient data assimilation over land. The tangent-linear adjoint model is neither available in the current operational CRTM. Therefore, the MPLSEM in the current operational CRTM is only able to provide forward emissivity simulations, without the function to support the radiance data assimilation of the surface control variables.

The MPLSEM tangent-linear and adjoint models have been recently implemented in the Version 1.0 package of the Community Surface Emissivity Models (CSEM) system (Chen et al. 2016). CSEM Version 1.0 will replace the existing CRTM surface modules in the next CRTM major release 3.0. The tangent-linear adjoint function of MPLSEM will enable us to perform land surface radiance data assimilation with CRTM.

We have also made a lot of efforts to optimize the MPLESEM performance so that we may make use of its potential in land surface radiance data assimilation. With a long list of model parameters, the optimization and calibration of the MPLSEM proved to be very challenging at global scale. While working on the MPLSEM optimization, we identified another feasible approach to develop a prognostic model similar to MPLSEM in functionality, but with much higher accuracy for applications at global scale. This model is based on machine learning of the "physical" mechanism from satellite instantaneous observations. The first version of this machine-learning based model has been recently developed. The model performance appears very promising based on several real case studies. In this article, we briefly introduce the latest advance in the related efforts. The model together with some preliminary analysis results are introduced in the next sections.

Data and Method

The Earth's surface emissivity depends on surface dielectric compositions and surface scattering properties, which vary substantially in space and time over land. It is assumed in the MPLSEM that surfaces with similar soil texture and vegetation cover have similar radiative property. For a specific vegetation and soil combination, the real-time media dielectric property are determined by vegetation cover fraction, leaf area index, soil moisture content, soil temperature, and land skin temperature, which brings out the real time surface emissivity output.

With a long list of model parameters, the calibration of the MPLSEM proved to be very challenging at global scale. As the result, it is found that it has limited capability to characterize the spatial variations of different surface cover types, resulting in very inefficient data assimilation over land. Shown in ***Figure 1*** are the MPLSEM emissivity map at NPP ATMS 23.8 GHz channel and the corresponding emissivity retrievals from instantaneous ATMS observations. Note that the instantaneous emissivity retrieving can only be performed under non-scattering condition. In average, there is only about 20% clear-sky coverage globally each day (https://isccp.giss.nasa.gov/role.html). So the instantaneous emissivity retrieval map is a collection of all the available the instantaneous retrievals of August 2018. Obviously, the MPLSEM is not able to produce the similar spatial patterns shown in both the instantaneous retrievals. The MPLSEM emissivity also appears too high, especially over bare soil and desert regions. Despite of the large bias at large spatial scale, it is expected that the MPLSEM may retain the reasonable temporal variation at individual sites (e.g.,

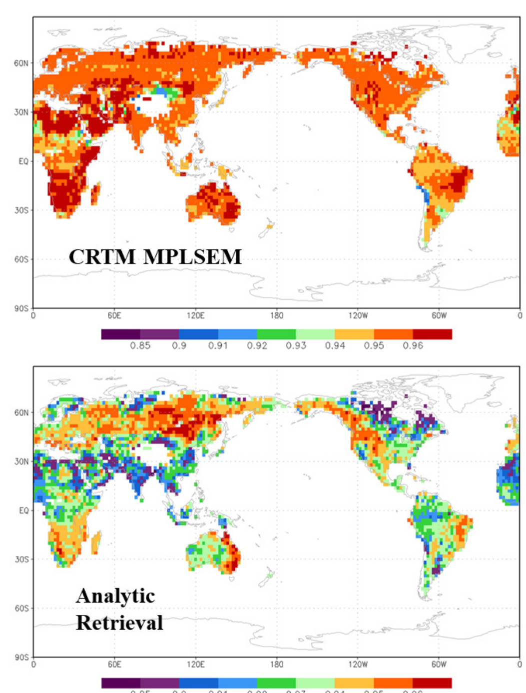

Figure 1. *Emissivity map simulated with the CRTM MPLSEM at NPP ATMS 23.8 GHz channel and the corresponding emissivity retrievals from instantaneous ATMS observations.*

the diurnal changes), which is essential for numerical weather data assimilation.

Microwave observations of satellite window channels are strongly affected by the underlying surface conditions. So, in contrast to the physical estimation of surface emissivity, emissivity may be obtained by the best fitting to the instantaneous satellite observations provided that the atmospheric contributions could be properly removed. Our new model begins with the same general assumption as the physical model: similar land surfaces should have similar radiative property, meaning that some unique mechanism relationship should hold between surface emissivity and the surface sate variables for a specific surface type. If this is right, such relationship should be contained in the related data, too. Emissivity retrievals based on instantaneous satellite window-channel observations have the best correlation with the real-time surface conditions. As an initial effort, we prepared two months of instantaneous emissivity retrievals with the ATMS observations (08/2018 and 09/2018). The retrieving was performed in NOAA GSI, where the collocated surface state parameters are available and recorded. The acquired data were then stratified by the surface vegetation cover types. The global surface cover type data is exactly the same as that used by the MPLSEM.

To explore the dynamic or "mechanism" relationship between surface emissivity and the independent surface state parameters (a prognostic model), we performed multilayer perceptron machine leaning over the independent state vector space for each individual surface cover type. The independent state vector space is similar to that used by the MPLSEM, which consists of six dimensions: frequency, zenith angle, vegetation cover fraction, land skin temperature, soil temperature and soil moisture content. The multilayer perceptron is a four-layer artificial neural network with one input layer, one output layer and two nonlinear hidden layers. The number of neurons varies for different land cover types, but it is normally about 25 for the first hidden layer.

Only part of the total data samples were used in the training, which enables us to check whether the established model is not only valid in the training space, but also retains certain generality and may be applicable for the rest of non-trained data samples. The results turned out to be very promising as shown in the following.

Preliminary Result Analysis

Shown in ***Figure 2a*** is the scatter plot of the emissivity reconstructed with the machine-learning (ML) based model over the training data space. The surface cover type is scrub grassland (Type 7). 4,900 out of total 56,000 data samples (about 8.7%) were used in the training, which evenly distributed over the independent parameter vector space. The mean value of the ML-based emissivity minus the analytic instantaneous emissivity retrieval in the training data space is less than 10-6, and the standard deviation is 0.00652. It is not surprising to have such a good accuracy and precision in the training data space. As argued earlier, the objective of our effort is to establish a prognostic model over the surface independent parameter space. So the model generality is our primary concern. To verify the generality of the ML-based model, we first apply it to the rest 91% data samples that were not used in the training. ***Figure 2b*** is similar to ***Figure 2a*** but for the non-trained data samples

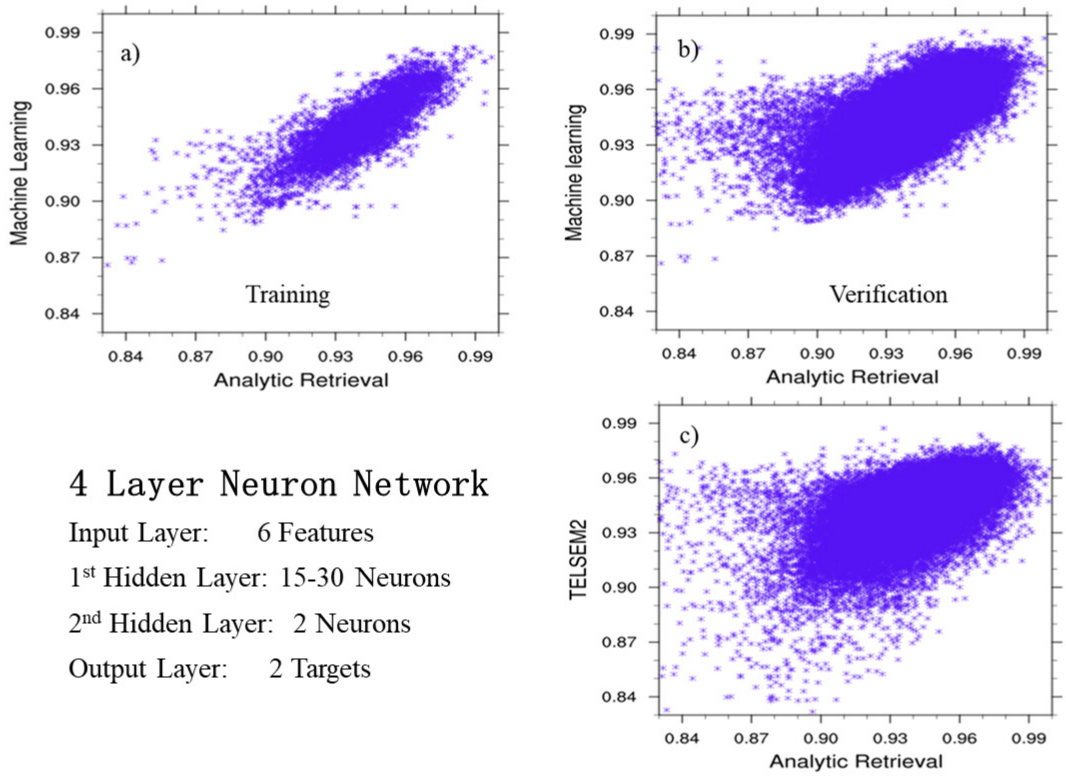

Figure 2. *The scatter plots comparing the ML-based emissivity, the instantaneous analytic retrieval, and the TELSEM monthly mean emissivity: A) Analytic Retrieval Vs ML-based in the training data space b) Analytic Retrieval Vs ML-based in the non-trained data space c) Analytic Retrieval Vs TELSEM.*

of scrub grassland type. The mean emissivity difference (ML-based minus retrieval) is now 0.0063, and the standard deviation is 0.0018. Obviously, the accuracy (mean difference) of the ML-based model is degraded when applied in non-trained data space. The accuracy degradation is understandable, but in a very acceptable range. The standard deviation (precision) even becomes better in the non-trained data space. This actually results from the lower percentage of the "outliers" in the non-trained data space. For the purpose of comparison, a similar analysis is performed with the monthly TELSEM emissivity and is shown in ***Figure 2c***.

Similar results were obtained for all the other surface cover types. Shown in ***Figure 3b*** is the global ML-based emissivity maps (including all surface cover types) built at ATMS 23.8GHz channel on the non-trained data space, which agrees very well with the analytic instantaneous emissivity retrievals ***(Figure 3a)*** in spatial variation details. For the purpose of comparison, the TELSEM (Aires et al. 2011) monthly mean atlas is also shown ***Figure 3c***. All the three data maps show consistent spatial variations, indicating that they have very comparable quality at global scale.

Conclusion and Further Work

The strength of a physical model is obvious, providing dynamically varying emissivity and is physically based. Yet its downside is also obvious with a long list of the model parameters and the complex mechanism. By contrast, the ML is statistically straightforward with the multilayer neural network architecture and advanced nonlinear programming. If data quality is carefully controlled and sufficient samples are available, a fine-tuned ML is able to effectively capture the "mechanism" relationships similar to the physical model. The prognostic land surface

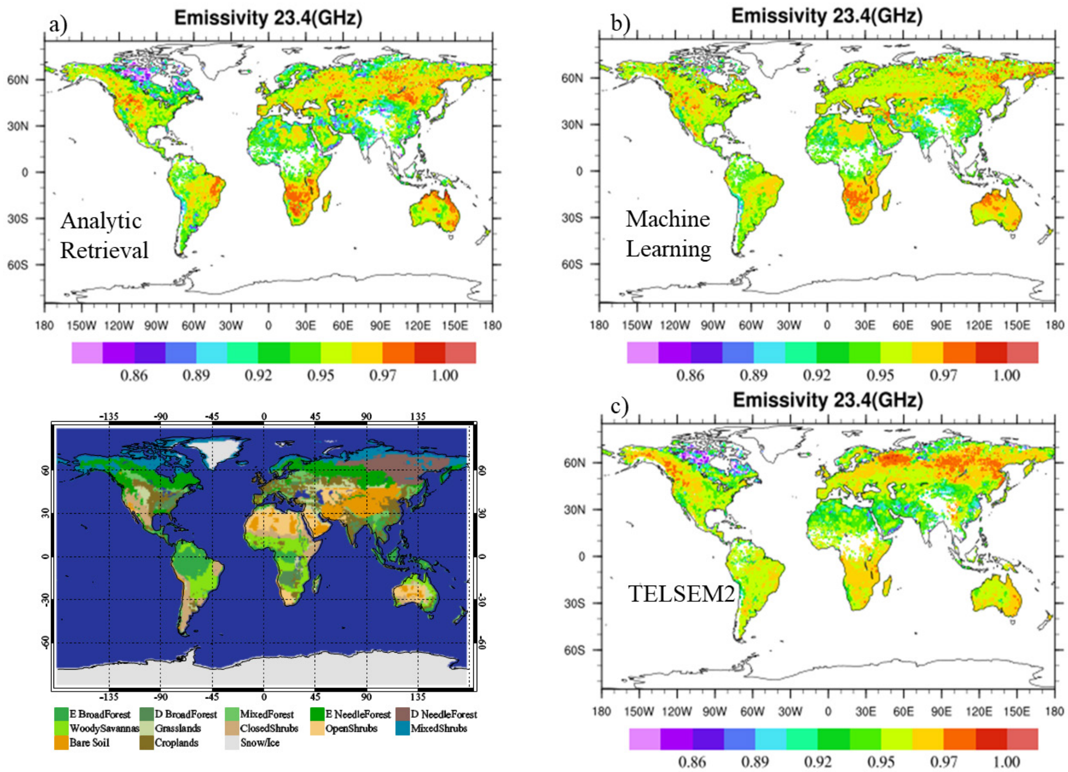

Figure 3. *Emissivity map a) retrieved from NPP ATMS instantaneous observations; b) simulated with the ML-based prognostic model; c) and the TELSEM monthly mean atalas.*

emissivity model based on machine learning shows very consistent performance over different land surfaces. In contrast with the static emissivity retrievals, the ML-based emissivity model has the prognostic capability once established. Comprehensive verification testing is ongoing with more real case studies. We also need more training data sets from different sensor observations to consolidate the model generality. Currently, the model was only trained for use with warm season cases. The land surface radiative property may experience significant changes in cold seasons, so more training and verification efforts will be performed for cold seasons. To improve the model accuracy and the model generality, we also need to refine the artificial neuron network architecture and the nonlinear optimization algorithms.

Authors

Ming Chen (CICS-ESSIC/UMD), Kevin Garrett (STAR/NESDIS), and Yanqiu Zhu (I.M. Systems Group at NCEP/EMC)

References

Weng, F., B. Yan and N. Grody, "A microwave land emissivity model", *J. Geophys. Res.*, vol. 106, NO. D17, pp 20,115-20,123, 2001.

Chen M., and F. Weng, "Modeling Land Surface Roughness Effect on Soil Microwave Emission in Community Surface Emissivity Model", *IEEE. Trans. Geosci. Remote Sens.*, 54(3), 1716-1726, 2016.

Aires, F., C. Prigent, F. Bernardo, C. Jimenez, R. Saunders and P. Brunel, "A Tool to Estimate Land-Surface Emissivities at Microwave frequencies (TELSEM) for use in numerical weather prediction," *Q. J. R. Meteorol. Soc.*, 137: 690-699, 2011.

Chen M., F. Weng, "Development and Improvement of Community Surface Emissivity MODEL (CSEM) system," 4th RSMSP, Grenoble, France, 2016.

PEOPLE

Welcome Dr. Mark Olah

Dr. Mark J. Olah joined the JCSDA in May 2019, as a Software Engineer with the JEDI core team. Primarily, Dr. Olah is focused on the automation of observation processing, data assimilation workflows, and cycling forecast systems in cloud-computing and HPC environments. He has extensive experience in designing object-oriented parallel data processing toolchains for a wide range of scientific applications that he brings to the JEDI project.

Mark has bachelor's degrees in Computer Science and Mathematics from Carnegie Mellon University, where he worked on advanced mesh generation and refinement algorithms for Navier-Stokes fluid flow simulations using a fully-Lagrangian framework and nonlinear mesh elements. Mark received his PhD in Computer Science from the University of New Mexico in 2012, where his research focused on parallel simulations of nano-scale molecular robots using a combination of stochastic simulation of individual chemical binding reactions together with Markov-chain Monte Carlo estimates of thermal motion and equilibria.

After graduation, Mark's postdoctoral work focused on machine learning and optimization algorithms in microscopy applications involving single-molecule localization and tracking. As part of this project, Mark designed a complete C++/OpenMP based single-molecule data processing toolchain and associated Matlab GUI applications to track individual fluorescently-labeled molecules in video data, allowing precise scientific inferences for cell-biology applications.

Outside of work, Mark's interests are in exploring the Rocky Mountains by foot, bike, raft, snowshoe, and ski. Mark and his wife, Samantha, have climbed over 500 mountains across the western U.S., and (if you know where to look) can be found off-trail in seldom visited mountain basins and on the summit of peaks with no name.

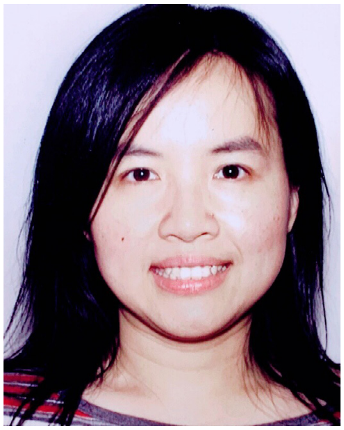

Introducing Dr. Emily Liu

Dr. Emily Liu joined the New and Improved Observation (NIO) team at UCAR/JCSDA in August 2019, as a project scientist. Her primary responsibility and focus are towards advancing the use of satellite data in data assimilation systems, as well as exploring the use of new and improved satellite observations. These tasks are largely related to her past work experience at NASA GMAO and NOAA NCEP where she obtained extensive training and skills.

Emily is originally from Taiwan. To pursue her interests in science, she attended the University of Wisconsin-Madison for where she earned two master's degrees in atmospheric science and mechanical engineering. She then obtained her PhD in atmospheric science studying the relationship among dynamic cloud microphysics and radiation in cirrus clouds using a numerical model. After one year of postdoctoral experience, she joined NASA GMAO to work on assimilating satellite data into a data assimilation system for weather forecasting and reanalysis for climate prediction, which was a completely new direction from her dissertation that later became her main interest. In recent years, she worked at NOAA NCEP to continue her interest in using satellite radiances under all-sky conditions and in the validation and improvement of radiative transfer models for data assimilation applications.

In her free time, Emily enjoys playing piano and flute, sketching, watching movies, and playing basketball. She is a cat lover and enjoys working as a volunteer in animal shelters.

Say Hello to Mr. Philip Gibbs

Philip Gibbs joined the JCSDA in Boulder Colorado as Executive Officer in April 2019. In this role, he leads the coordination of all projects that make up the JCSDA program and works directly with director, Tom Auligne.

Philip brings to the program more than 15 years of project management and system engineering experience having worked in the fields of radio astronomy and electronic research. Originally from Cape Town South Africa, he worked on the design and construction of the MeerKAT Radio Telescope before joining the international Square Kilometre Array (SKA) project office situated south of Manchester in the United Kingdom. During the five years he spent leading the design phase of the SKA telescope involving global academic institutions and partner organizations, Philip developed the skills and tools required to achieve successful outcomes in scientific research projects, a discipline well suited to the vision of the JCSDA program.

Out of the office, Philip spends time climbing with his daughter and exploring the plethora of Rocky Mountain bike trails with his son. Nervously excited about the coming snow season, Philip is keen to see if his passion for watersports and surfing will stand him in good stead to take on the slopes of the Colorado mountains. Time will tell…watch this space!

Welcome Dr. Ryan Honeyager

Ryan Honeyager joined the JCSDA in July 2019, as a member of the Joint Effort for Data Assimilation Integration (JEDI) team. Initially, he is working on improvements to the Unified Forward Operator (UFO) code with the longer-term goal of preparing JEDI for operational use with NOAA-EMC products. He is the liaison to NOAA EMC in College Park, MD.

Ryan earned his PhD and MS degrees in Meteorology from Florida State University. His research focused on modelling radiative properties of snow and connecting models of ice clouds and precipitation with observations. This work led to participation in the NASA Convective Processes Experiment (CPEX) field campaign, as well as a few cool (in his opinion) studies of convective and stratiform precipitation. He is assembling the International Precipitation Working Group (IPWG)'s white paper on scattering table standardization, which feeds into the CRTM, RTTOV, and ARTS radiative transfer models.

In 2018, Ryan moved to the District of Columbia and joined the NOAA Microwave Integrated Retrieval System (MiRS) team. While there, he developed machine learning-based products for the remote sensing of snow and ice, and he also made various improvements to MiRS' internal architecture.

Apart from science, Ryan loves cooking, dogs, hiking, history, running, theatre, and traveling.

EDITOR'S NOTE

It is a pleasure to share the Fall 2019 JCSDA Newsletter. I think you will find this issue to be uniquely interesting and informative, as the three science articles comprising the heart of this edition are organized not so much around a single project or area, but instead provide a reminder of the breadth of the applications and systems that the JCSDA pursues through and for its partners and the larger science community.

For example, in one article, John McMillen describes the Prediction and Data Assimilation for Cloud (PANDA-C) development sponsored by the US Air Force, on which the JCSDA JEDI team and other partners are developing a cloud DA system to support improved forecasting, utilizing collaborative practices for SW development. This work not only addresses the focused cloud prediction needs of the Air Force, but also has provided a proving ground for the application of JEDI-to-model interfacing and the use of other JEDI components as well as elements of the CRTM.

In another piece, Erica McGrath-Spangler and co-authors from NASA report on the use of adaptive thinning of cloud-cleared AIRS radiances in NASA's global forecast model. In their work they address some of the short-comings of standard approach to using hyperspectral IR radiances, including the under-sampling of critical meteorologically active and cloud-impacted regions including high latitude areas and in the tropical cyclone environment. Their results suggest encouraging possibilities for improved forecasting in all JCSDA partner NWP systems, extending beyond AIRS to CrIS and IASI.

Ming Chen of NOAA/NESDIS describes recent efforts to reap the scientific advantages of the Microwave physical land surface emissivity model (MPLSEM) in practical application, where the multitude of model parameters and the complexity of their interaction can impede reaping the gains of a realistic physics-based dynamic approach. Using a machine learning approach, the early results appear to be promising.

Since the last issue, several important staffing vacancies have been filled for the JCSDA. In this newsletter, you can learn a little about Ryan Honeyager, Phillip Gibbs, Mark Olah, and Emily Liu – the work they are doing, their professional backgrounds, and how they occupy their time away from their workstations. As always, I encourage you to give them a warm welcome to the JCDSA when you meet them, to help them as come on board, and to take advantage of the talent and energy they bring to our mission.

Finally, I remind you to review the calendar of upcoming events, as there is something of interest for almost everyone there. In particular, I hope that I will see many of you in Boston, MA in January for the JCSDA Symposium as part of the 100th Annual Meeting of the American Meteorological Society (AMS.)

Jim Yoe

SCIENCE CALENDAR

UPCOMING EVENTS

MEETINGS OF INTEREST

DATE	LOCATIONS	WEBSITE	TITLE
October 31–November 6	Saint-Saveur, Québec, Canada	https://cimss.ssec.wisc.edu/itwg/index.html	TOVS ITSC The 22nd International TOVS Study Conference (ITSC-22)
November 4–8, 2019	Herzliya, Israel	http://www.cospar2019.org/	4th COPSAR Symposium Small Satellites for Sustainable Science and Development
December 9–13, 2019	San Francisco, CA	https://sites.agu.org/	AGU
January 12–16, 2020	Boston, MA	https://www.ametsoc.org/index.cfm/ams/	AMS Annual Meeting
June 8–12, 2020	Fort Collins, CO	https://www.cira.colostate.edu/conferences/8th-international-symposium-on-data-assimilation/	8th International Symposium on Data Assimilation (ISDA)

MEETINGS AND EVENTS SPONSORED BY JCSDA

DATE	LOCATIONS	WEBSITE	TITLE
February 24–27, 2020	Monterey, CA	https://www.jcsda.org/events/2020/2/24/4th-jedi-academy	JEDI Academy 4
February 28, 2020	Monterey, CA	https://www.jcsda.org/events/2020/2/28/crtm-training-amp-user-workshop	CRTM Workshop
February 3–5, 2020 8:00AM–5:00PM	Reading, United Kingdom	https://www.ecmwf.int/en/learning/workshops/4th-workshop-assimilating-satellite-cloud-and-precipitation-observations-nwp	Joint Workshop JCSDA & ECMWF

CAREER OPPORTUNITIES

Opportunities in support of JCSDA may be found at https://www.jcsda.org/opportunities as they become available.